Applied Catalysis B: Environmental 88 (2009) 351–360

Contents lists available at ScienceDirect

Applied Catalysis B: Environmental

journal homepage: www.elsevier.com/locate/apcatb

A crucial role of O_2^- and O_2^{2-} on mayenite structure for biomass tar steam reforming over $Ni/Ca_{12}Al_{14}O_{33}$

Chunshan Li *, Daisuke Hirabayashi, Kenzi Suzuki

EcoTopia Science Institute, Nagoya University, Nagoya 464-8603, Japan

ARTICLE INFO

Article history:
Received 29 July 2008
Received in revised form 30 October 2008
Accepted 1 November 2008
Available online 17 November 2008

Keywords:
Biomass tar
Toluene steam reforming
$Ni/Ca_{12}Al_{14}O_{33}$
Coke-resistance
Sulfur poisoning

ABSTRACT

Newly synthesized nickel calcium aluminum catalysts ($Ni/Ca_{12}Al_{14}O_{33}$) were tested in a fixed bed reactor for biomass tar steam reforming, toluene as tar destruction model compound. Four catalysts ($Ni/Ca_{12}Al_{14}O_{33}$) were prepared with Ni loading amount from 1, 3, 5 to 7 wt%, even 1% loading catalyst also showed excellent performance. Catalysts aged experiments in the absence (60 h on stream) and presence of H_2S were characterized by BET, X-ray diffraction (XRD), and Raman spectra. It was observed that $Ni/Ca_{12}Al_{14}O_{33}$ showed excellent sustainability against coke formation due to the "free oxygen" in the catalysts. It also exhibited higher H_2S-poisoning resistance property compared to the commercial catalysts Ni/Al_2O_3 (5%) and $Ni/CaO_{0.5}/MgO_{0.5}$. Raman spectra revealed that "free oxygen O_2^- and O_2^{2-}" in the structure of the catalysts could be substituted by sulfur then protected Ni poisoning on some degree, but reactivation experiments by O_2 flowing showed that the sulfide $Ni/Ca_{12}Al_{14}O_{33}$ was difficult to completely restore, incorporation of sulfur in the structure only partly regain by O_2. The kinetic model proposes, as generally accepted, a first-order reaction for toluene with activation energy of 82.06 kJ mol^{-1} was coincident with the literature data. The $Ni/Ca_{12}Al_{14}O_{33}$ catalyst was effective and relative cheap, which may be lead to reduction in the cost of hot gas cleaning process.

© 2008 Elsevier B.V. All rights reserved.

1. Introduction

Fossil fuel reserves are diminishing rapidly across the world, the need for renewable alternatives is becoming more urgent. The utilization of biomass is getting increased attention as an abundance and cheap source of renewable energy. Among them, biomass gasification has attracted huge interest by producing a gas rich in H_2 and CO used for fuel directly, or methanol [1,2]. Unfortunately, producer gas from this process usually contains unacceptable levels of tar, which can cause operational problems in downstream processes by blocking gas coolers, filter elements and engine suction channels. Most producer gas applications also require removal of at least part of the dust and tar before the gas can be used. Hence, the tar control and convert is a key issue for a successful application of biomass derived producer gas.

The catalytic steam reforming is a very attractive technique for biomass gasification and tar removal. Several kinds of catalysts were studied, developed and used in this process, such as mineral, Ni-based and noble metal catalysts. Duprez gave the summary of metal catalysts on steam reforming of aromatic compounds [3]. During biomass gasification process, hydrocarbons reforming are the main reactions, among which nickel catalysts were the most popular and effective, used commercially for more than 40 years. During biomass gasification process, complex hydrocarbons steam reforming reactions are included, which involves a risk of carbon deposition, then may reduce the performance of the catalyst in several ways, and it may eventually have to be replaced. So carbon formation is regarded as one main problem for deactivation of Ni-based catalysts. Deactivation by sulfur is another one. Product gas formed from biomass gasification process contains the major components CO, H_2, CO_2, CH_4 and H_2O, in addition to organic (tars) and inorganic (H_2S, HCl, NH_3, alkali metals) impurities and particulates. Even after a thorough desulfurization of the process, sulfur containing compounds may reach the nickel catalyst at a ppb level, which is also a strong poison concentration for nickel catalysts and blocks nickel active sites. So the combination of high temperatures, the presence of hydrocarbons, high-pressure steam and sulfur containing compounds creates a severe environment for nickel catalysts, the nickel steam reforming catalysts will encounter four challenges: activity, sulfur poisoning, carbon formation and sintering [4].

Several attempts have been made to enhance the sulfur tolerance and decrease in carbon formation by modifying the preparation methods [5–8], adding accessory ingredient such as noble metal [9–22] or alkali [23–25]. Nikolla et al. [5] proved that

* Corresponding author. Tel.: +81 52 7895845; fax: +81 52 7895845.
E-mail address: li_chunshan@nagoya-u.jp (C. Li).

0926-3373/$ – see front matter © 2008 Elsevier B.V. All rights reserved.
doi:10.1016/j.apcatb.2008.11.004

the carbon tolerance of Ni could be improved by synthesizing Ni-containing surface alloys comparing to monometallic Ni. Plasma treated Ni/Al_2O_3 catalyst exhibited high catalytic activity and excellent resistance to the formations of filamentous carbon and encapsulating carbon [6]. A 1 wt%/0.5 wt% nickel/calcium catalyst, co-precipitated inside porous filter discs using the urea method to improve the resistance of the catalyst against sulfur poisoning was found [7]. Ni/dolomite developed by special method showed high activity and gave negligible carbon deposition comparing to conventional supported Ni catalysts [8]. Adding noble metals such as Ru [9–11], WO_3 [12,13], Pt [14–16], Rh [17–19], Pd [20], Mn [21] for promoting the catalyst property was also studied. For example, A catalyst consisting of Ru (5%) dispersed on 15% MgO/Al_2O_3 carrier exhibited high activity and selectivity on steam reforming aqueous fraction of bio-oil, as well as satisfactory stability with time on stream, only a small part of the deposited carbon on the catalyst surface was found [8]. Newly developed Ni/MgO–CaO catalyst doped with WO_3 showed high naphthalene reforming activity and exhibited superior resistance to carbon formation [12]. Fabrication of nominally doped nano-scale ceria-supported palladium catalyst matrices also showed good sulfur-tolerant [20]. However, Ru, Rh, Pt are prohibitively expensive [22], which results in no practical application as industrial catalysts. Concerning the effect of alkali on the formation of carbon was also studied [23–25]. Promotion with potassium and effect of water on alumina-supported nickel catalysts was studied by Demicheli et al., and the main variables affecting the kinetics of carbon formation was also established [23]. The effect of K loading (1–3 wt%) on catalytic, stability and coking rate for steam reforming of ethanol have been addressed by Frusteri et al., K addition stabilizes Ni catalyst mainly by depressing the metal sintering [24]. Results of the investigation suggest that stable Ni/Al_2O_3 catalysts for the carbon dioxide reforming of methane can be prepared by the addition of both potassium and CeO_2 (or MnO) as promoters [25].

Mayenite ($Ca_{12}Al_{14}O_{33}$) was previously developed and used in our group, proved that it had high performance on hydrocarbon catalytic combustion because of its high oxygen restored property [26,27]. In this study, newly synthesized nickel based mayenite catalysts ($Ni/Ca_{12}Al_{14}O_{33}$) by solid mixing method were tested for biomass tar steam reforming. The concentration of Ni metal in the catalysts from 1, 3, 5 to 7% were prepared. Catalysts aged experiment (60 h on stream) showed negligible carbon formation and excellent H_2S toleration property comparing to $Ni/MgO_{0.5}/CaO_{0.5}$ and Ni/Al_2O_3. Raman spectra revealed that sulfur-tolerant property lay in the "free oxygen" in the structure of the catalysts, which could be substituted by sulfur atom, and prolonged catalyst life. Lastly, activation energy of 82.06 kJ mol^{-1} for toluene steam reforming process was calculated by the proposed kinetic model.

2. Experimental

2.1. Catalysts

Mayenite ($Ca_{12}Al_{14}O_{33}$) was prepared by solid mixing of $Ca(OH)_2$ and $Al(OH)_3$ in stoichiometric ratio, grinding and calcination at 1000 °C over 4 h in air environment, followed by crushing and sieving to obtain particle sizes between 212 and 425 μm. The schematic structure is shown in Fig. 1. It has been described previously as a calcium-aluminate framework, in which 32 of the 33 oxygen anions are tightly bound, containing large cages, 1/6 of them being filled randomly by the remaining "free oxygen" [27]. $Ni/Ca_{12}Al_{14}O_{33}$ (Ni = 1, 3, 5, 7%) was prepared by mixing mayenite with NiO in different stoichiometric ratio, grinding without water, calcined at 600 °C in air environment, then crushed to the same size as mayenite. Ni/Al_2O_3 (5 wt%) and $Ni/CaO_{0.5}/MgO_{0.5}$ (5 wt% Ni, the mixture $CaO_{0.5}/MgO_{0.5}$(50/50 wt%) as support) were prepared by impregnation method with aqueous solution of nickel nitrate hexahydrate followed by drying at 120 °C overnight, then calcined at 800 °C for 4 h, used for represent the commercial catalyst.

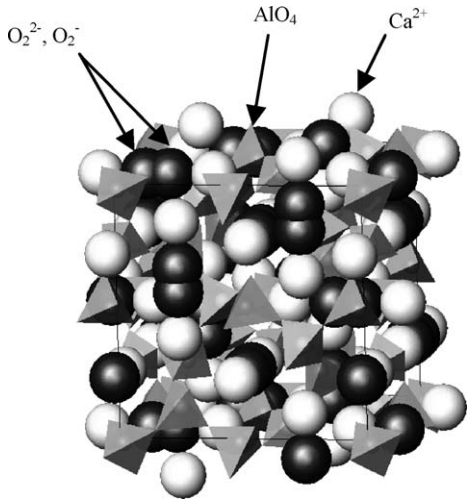

Fig. 1. Schematic drawing of mayenite. (Each AlO_4 is three dimensionally linked with one another by sharing corner oxygen atoms. 'Free' oxygen is located in micro-pores of mayenite.)

X-ray powder diffraction was taken with Mac Science M18 XHF-SRA XRD apparatus with Ni-filtered Cu Kα radiation. The acceleration voltage was 30 kV and the acceleration current was 100 mA. Raman spectroscopy was taken by NRS-1000 spectrometer with the 532.30 nm excited line of an Ar^+ green laser. Scanning range is 700–1200 cm^{-1}. The BET surface area was measure with a Belsorp II (BEL Japan, Inc.).

2.2. Apparatus and operation parameters

Experiments were carried out at atmospheric pressure in a fixed bed quartz reactor (10 mm I.D.). The scheme was shown in Fig. 2. All the catalysts were initially activated with the reduced gas mixture (<5% H_2 diluted by Ar) for 1.5 h at 650 °C, then tested at the given operation parameters. For the feed gas mixture, argon was used as the dilution gas, toluene was introduced by permeater (GasTec PD-1B) carried by Ar gas. In the presence of H_2S, the diluted gas was H_2S/Ar (500 ppm H_2S), the toluene concentration was around 4000 ppm in the feed (25 °C). Water was pumped by syringe into a vaporization furnace, then mixed with toluene/argon gas. All the pipelines were kept around 120 °C.

2.3. Analysis

The reactant and product gases were analyzed simultaneously by two on-line gas chromatograph. Toluene, benzene and other organic compounds were analyzed by GC-FID with a silicone OV-1.2% (2.0 m × 3.0 mm I.D.) packed column. The products gases (H_2, CO, CO_2, CH_4) were analyzed by GC-TCD with a packed carbon sieve column (2.0 m× 3.0 mm I.D.).

To determine the catalytic activity of the Ni/mayenite, the toluene conversion and products composition in the fixed bed were studied. Toluene conversion, H_2 yields and the selectivity of CO_2, CO, benzene, CH_4 were calculated with formulae (1), (2) and (3), respectively.

Toluene conversion, X_c, can be defined as Eq. (1):

$$X_c = \frac{C_{T,in} - C_{T,out}}{C_{T,in}} \times 100 \quad (1)$$

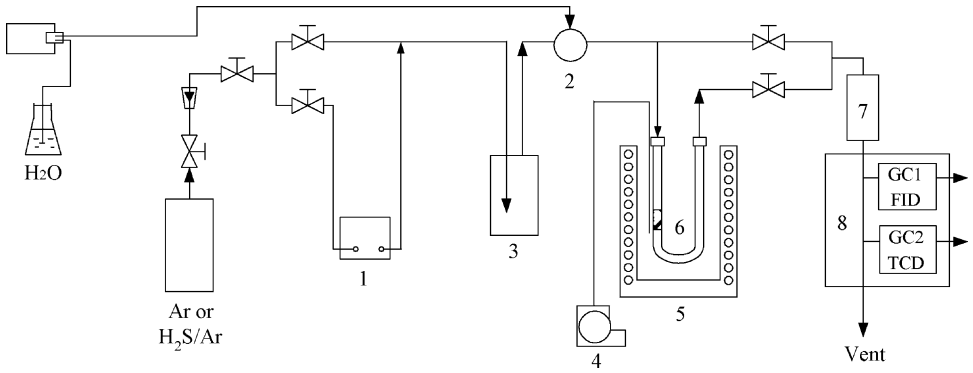

Fig. 2. Experimental scheme for toluene steam reforming: (1) Permeater, (2) vaporization furnace, (3) bumper, (4) thermocouple, (5) furnace, (6) reactor, (7) dryer system and (8) analysis system.

$C_{T,in}$ and $C_{T,out}$, respectively: toluene molar concentration of the inlet and outlet gases.

Hydrogen yield, Y_{H_2} Eq. (2), is expressed as the percentage of the stoichiometric potential corresponding to the total conversion of toluene according to reaction (6).

$$Y_{H_2}\,(\%) = \frac{[C_{H_2}]_{out}}{18[C_{T,in} - C_{T,out}]} \times 100 \quad (2)$$

The carbon containing products (CO, CO_2, CH_4) are calculated by the selectivity S_i (Eq. (3)), which are defined as the ratio of the amount of carbon in the product i to the amount of carbon in the reacted toluene.

$$S_i = \frac{[C_i]_{out}}{7[C_{T,in} - C_{T,out}]} \times 100 \quad (3)$$

$[C_i]$: molar concentration of i = CO, CO_2 and CH_4

The selectivity of benzene S_B is calculated by Eq. (4).

$$S_B = \frac{[C_B]_{out}}{[C_{T,in} - C_{T,out}]} \times 100 \quad (4)$$

$[C_B]$: molar concentration of benzene in the products.

3. Results and discussion

In order to study the catalytic activity of the Ni/mayenite on the effect of operation parameters (reaction temperature, S/C ratio and space-time), toluene steam reforming was performed with the Ni/mayenite in the absence and presence of H_2S two conditions. For all experiments before steam reforming reaction, the catalyst is reduced by H_2 (<5% diluted by Ar) for 1.5 h at 650 °C.

Many parallel and consecutive reactions can take place during steam reforming [3], so the final products can be regarded as the results from the competition of these reactions. Different operation conditions such as S/C, temperature, and catalysts will result in different products. These gases yield evolutions in the different condition can be explained by the following reactions involved in toluene steam reforming.

Steam reforming:

$$C_7H_8 + 7H_2O \rightarrow 7CO + 11H_2 \quad \Delta H_{(800\,^\circ C)} = 927.2\,kJ\,mol^{-1} \quad (5)$$

$$C_7H_8 + 14H_2O \rightarrow 7CO_2 + 18H_2 \quad \Delta H_{(800\,^\circ C)} = 688.5\,kJ\,mol^{-1} \quad (6)$$

Water gas shift

$$CO + H_2O \rightarrow CO_2 + H_2 \quad \Delta H_{(800\,^\circ C)} = 34.1\,kJ\,mol^{-1} \quad (7)$$

Dry reforming

$$C_7H_8 + 7CO_2 \rightarrow 14CO + 4H_2 \quad \Delta H_{(800\,^\circ C)} = 1166.0\,kJ\,mol^{-1} \quad (8)$$

Hydrodealkylation

$$C_7H_8 + H_2 \rightarrow C_6H_6 + CH_2 \quad \Delta H_{(800\,^\circ C)} = -50.9\,kJ\,mol^{-1} \quad (9)$$

Steam dealkylation

$$C_7H_8 + H_2O \rightarrow C_6H_6 + CO + 2H_2 \quad \Delta H_{(800\,^\circ C)} = -174.8\,kJ\,mol^{-1} \quad (10)$$

$$C_7H_8 + 2H_2O \rightarrow C_6H_6 + CO_2 + 3H_2 \quad \Delta H_{(800\,^\circ C)} = 140.7\,kJ\,mol^{-1} \quad (11)$$

Methane steam reforming

$$CH_4 + H_2O \leftrightarrow CO + 3H_2 \quad \Delta H_{(800\,^\circ C)} = 225.7\,kJ\,mol^{-1} \quad (12)$$

Other reactions such as carbon formation reaction by toluene decomposition and cracking also are included in the process.

3.1. Characterization of catalysts

Scanning electron microscopy (SEM) of mayenite (Fig. 3(a)) and Ni/$Ca_{12}Al_{14}O_{33}$ (5%) (Fig. 3(b)) showed porosity of the two catalysts (holes of diameters less than 1 μm). A deposit of almost spherical uniform grains (probably NiO) with size between 0.1 and 0.3 μm could be observed and hid completely the surface of mayenite for Ni/$Ca_{12}Al_{14}O_{33}$ from Fig. 3(b). Table 1 listed the basic physical properties before and after reaction, which also showed mayenite and Ni/$Ca_{12}Al_{14}O_{33}$ had low surface area.

Fig. 4(a) illustrated XRD patterns of mayenite and Ni/$Ca_{12}Al_{14}O_{33}$ (before reduce) with various concentration of NiO. The enlarged Fig. 4(b) illustrated that the angle of Ni/$Ca_{12}Al_{14}O_{33}$ had small shift comparison to mayenite, which lay in the part substitution Al^{3+} by Ni^{2+} in the structure. But the mount of substitution was very small. For the NiO/$Ca_{12}Al_{14}O_{33}$, there were the obvious NiO peaks in the XRD pattern for the NiO concentration above 1%.

Fig. 5 showed Raman spectra of mayenite and Ni/$Ca_{12}Al_{14}O_{33}$ before reaction. The Raman band at 1090 cm^{-1} was O_2^- species, and an additional band assignable to the O_2^{2-} species appeared at 880 cm^{-1}.

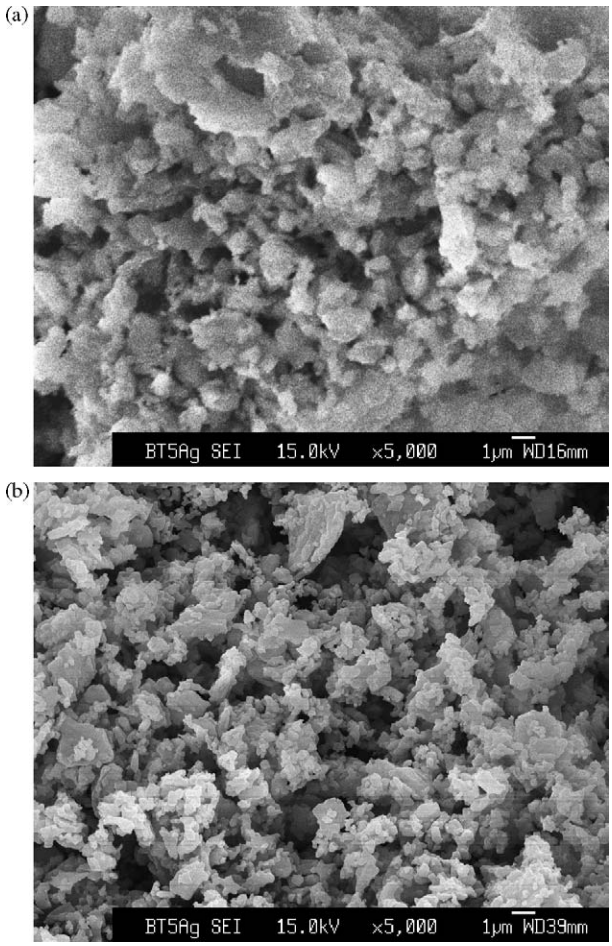

Fig. 3. Scanning electron micrographs of (a) mayenite and (b)Ni/mayenite (5%).

3.2. Steam reforming in the absence of H_2S

3.2.1. Reaction temperature

Experiment of steam reforming for toluene was carried out on mayenite and Ni/mayenite (1, 3, 5%) with a temperature range of 550–850 °C for a S/C ratio of 1.9 and space velocity of 6000 h^{-1} at 25 °C. No catalyst deactivation was observed after 24 h of time on stream. Toluene conversion on different catalysts was shown in Fig. 6.

From Fig. 6, Ni/mayenite exhibited excellent performance. For all Ni/mayenite catalysts, the toluene conversion reached nearly 100% at the temperature 750 °C, even though the concentration of Ni metal was only 1%. Results were compared to that obtained with mayenite alone (Fig. 6). The latter showed almost no activity (<6%) until 650 °C, moderate (50% at 800 °C) and weaker activity than with Ni/mayenite (5%) catalyst at 550 °C. And also for mayenite, additionally to CO, CO_2, and H_2, significant selectivity toward benzene (22% at 850 °C) are observed, but for Ni/mayenite, almost no benzene was observed. For toluene steam reforming, Świerczyński et al. [28] has also observed significant selectivity to benzene (6%) and polyaromatics (14%) on olivine, but Ni/olivine showed very low benzene selectivity. These results illustrated the importance of nickel in the selectivity and efficiency of catalyst during tar reforming.

In order to study the influence of temperature on products, Ni/mayenite (5%) was selected and the detail results of products were shown in Fig. 7. Below 600 °C, hydrogen yield increased quickly with reaction temperature. While trace benzene and CH_4 (<1%) (not shown in Fig. 7) were observed in the products in addition to H_2, CO and CO_2. Above 600 °C, nearly total toluene conversion to H_2, CO and CO_2 was available. But above 750 °C, the hydrogen yield associated with a decrease in CO_2 and an increase in CO was observed. The evolution of these results is due to a more important participation of the reverse water gas shift reaction (Eq. (7)), which is thermodynamically favorable at high temperatures. Comparison of our results with thermodynamic equilibrium curves revealed the agreement above 650 °C. Below this temperature, toluene steam reforming is governed by kinetics. Both thermodynamic equilibrium curve and our results (not shown in Fig. 7) give the benzene selectivity near to zero.

3.2.2. S/C influence

Studies of the effect of the S/C ratio on toluene steam reforming were performed for Ni/mayenite (5%) at 450, 500 °C. The space velocity was 6000 h^{-1} at 25 °C, and varied the steam flowrate to achieve the desired S/C ratios. The results were shown in Table 2. In the range of S/C from 1.4 to 2.6, obvious influence on toluene conversion (from 24.3 to 30.3% at 450 °C) was also observed. High S/C ratio resulted high toluene conversion, but high S/C ratio usually is not encouraged in industrialization process, because excess steam in gas products will reduce the quality of fuel and consume more energy.

The detail results obtained at 800 °C were presented in Fig. 8. H_2 and CO_2 yields increased but CO yield decreased when the S/C ratio increased. These gases yield evolutions with the S/C ratio can be explained by the reactions involved in toluene steam reforming (Eqs. (5)–(12)). Methane steam reforming was significantly affected by the S/C ratio, at high S/C ratio a very small amount of CH_4 was produced. The water gas shift reaction produced more H_2 and CO_2 at higher values of S/C ratios, so the increase in the CO selectivity at the same time less H_2 and CO_2 yield could be explained, a high steam partial pressure made the water gas shift equilibrium toward hydrogen formation. However, the partial pressure of the organic compound in the gas stream will be lower due to the dilution as the S/C ratio rise. All of those will affect the apparent kinetic constant.

3.2.3. Long-time evaluation

From the above results, Ni/mayenite (5%) exhibited excellent steam reforming activities of above 600 °C. To confirm the practical applicability of the promising industrialization catalyst, long-term durability test was conducted at the condition of 800 °C, space velocity of 6000 h^{-1} at 25 °C and inlet toluene concentration of

Table 1
The physical properties of mayenite and Ni/mayenite before and after reaction.

	Mayenite		Ni/mayenite (1%)		Ni/mayenite (3%)		Ni/mayenite (5%)	
	Before reaction	After reaction	Before reaction	After reaction	Before reaction	After reaction	Before reaction	After reaction
V_m (cm^3/g)	2.46	2.51	0.76	0.92	0.75	0.85	1.61	1.07
$a_{s,\ BET}$ (m^2/g)	10.7	11.8	3.3	4.0	3.3	3.7	7.0	4.6
The average diameter of hole (nm)	22.2	16.8	8.9	11.1	8.8	9.3	6.6	10.9

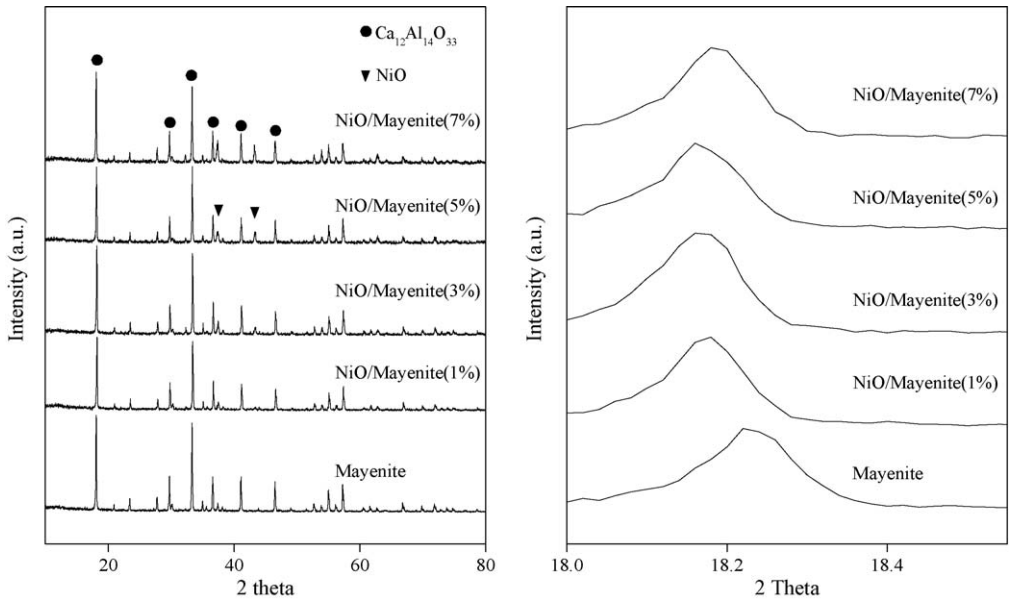

Fig. 4. X-ray diffraction pattern of mayenite and NiO/mayenite and enlarged.

4000 ppm, S/C is 1.15. The results were shown in Fig. 9, which illustrated Ni/mayenite maintain more than 98% of toluene reforming for more than 60 h at 800 °C, more stable than that of traditional Ni/Al_2O_3.

The observed promotion of catalysts such as dolomite, olivine by loading Ni metal for hydrocarbon reforming was justified, but also easily devitalized because of carbon formation on the nickel metal surface [29,30]. However, no obvious decrease of activation was observed for our catalyst based on the above results. At least three possible reasons to account for such unexpected observation may be considered. The first possibility is that the excess S/C ratio can prevent or reduce the formation of coke on the catalyst, especially the ratio above 1.2 [31], but the long-time evaluation of our experiments was carried out on the smaller S/C (1.15). A second possibility is that the formation of coke deposits on the surface of mayenite not nickel metal. In some cases, most of the formation of coke deposited on the supported surface, but only small amount on the activity component surface [32]. The quantitative analysis of coke amount on the after reaction catalyst performed with the TG analyzer (TGA, Rigaku Thermo Plus TG8120). The sample of 50–70 mg was heated from 30 to 1000 °C with a heating rate of 10 °C min^{-1} in air. The weight loss convincingly due to the combustion of deposited carbon less than 0.1% was observed, which indicated nearly no carbon deposition on Ni/mayenite.

For the third possibility is the "free" oxygen in the special structure of mayenite (Fig. 1), which was attributed to the presence of hydroxide, peroxide and superoxide radicals in the cages. So the superoxide radicals in the cages will transfer to nickel site to gasify the surface carbon on nickel metal to CO, which is the reasonable explanation for the excellent performance of Ni/mayenite [32].

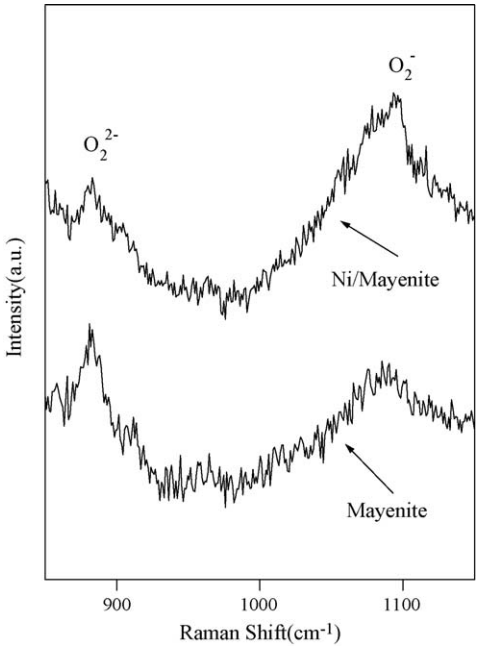

Fig. 5. Raman spectra of mayenite and Ni/mayenite before reaction.

3.3. Steam reforming in the presence of H_2S

The simulated biomass gasification sulfur containing for catalyst deactivation testing had following composition: toluene

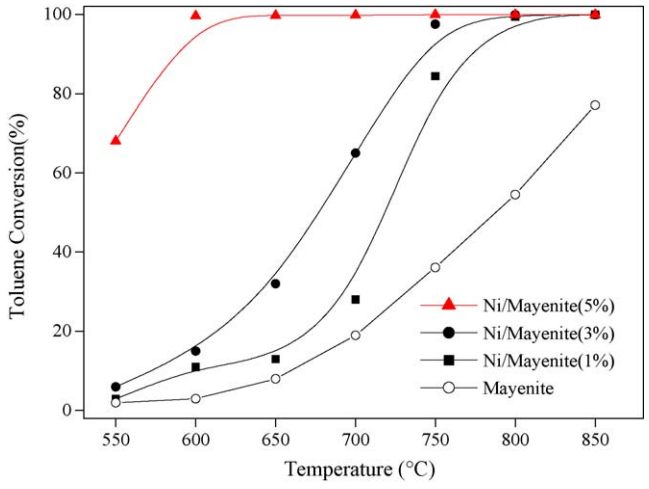

Fig. 6. Toluene conversion vs. temperature on mayenite and Ni/mayenite, (S/C = 1.9; *T*: 550–850 °C; S.V.: 6000 h^{-1}).

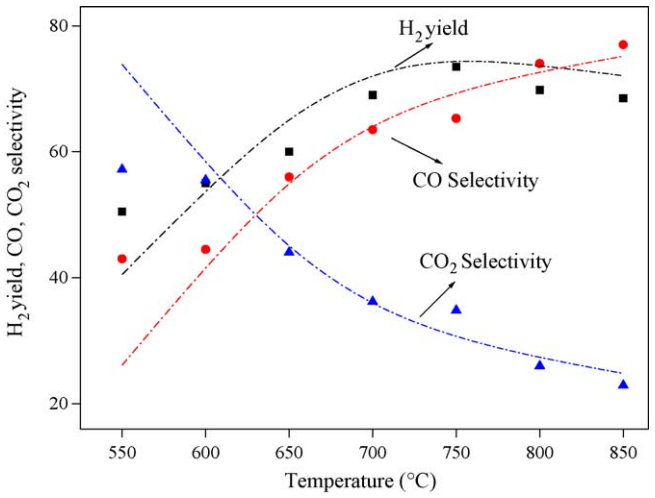

Fig. 7. The influence of reaction temperature on products composition for Ni/mayenite (5%) (S/C = 1.9, time on stream = 24 h, S.V.: 6000 h^{-1}).

4000 ppm, diluted by H_2S/Ar (H_2S: 500 ppm), appropriate steam was filled by syringe, At this condition, the model compound toluene and H_2S with a concentration of 4000 and 500 ppm, respectively was rather serious condition for biomass gasification gas.

3.3.1. Long-time evaluation

The effect of H_2S on the performance over Ni/mayenite (3 and 5%) was studied, and the results were compared to that of Ni/$CaO_{0.5}$/$MgO_{0.5}$ (5%) and Ni/Al_2O_3 (5%). The catalytic performance as a function of time was shown in Fig. 10. The activation decreased gradually and quickly for the Ni/Al_2O_3 (5%) and Ni/$MgO_{0.5}$/$CaO_{0.5}$ (5%) respectively, but for Ni/mayenite, the activation could be divided into two stages, under this reaction condition (H_2S: 500 ppm, the space velocity: 6000 h^{-1}), for the initial 60 min stage, the conversion and the products were similar with that of the absence of H_2S, but after this period, the toluene conversion decreased quickly, then kept almost constant above 70%. By analysis, the reasonable possibility to account for such unexpected observation is the "free" oxygen in the special structure of Ni/mayenite. We also studied the performance as a function of time under the same condition only increasing the space velocity from 6000 to 12,000 h^{-1}, it found that the conversion only remained around 30 min for the first stage, then decreased gradually. And

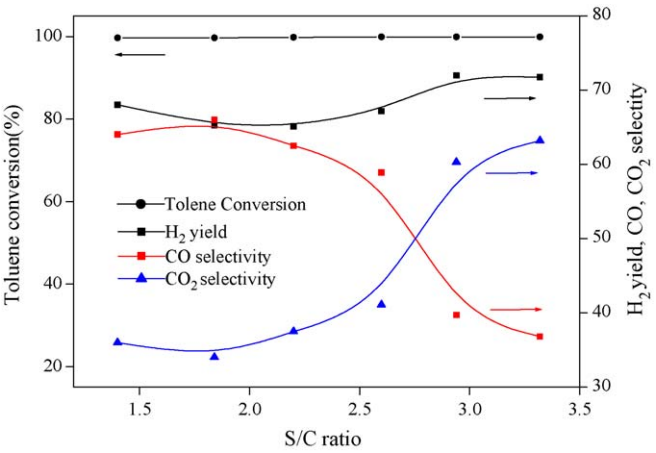

Fig. 8. The influence of S/C on toluene conversion and products composition for Ni/mayenite (5%) (temp.: 800 °C, S.V.: 6000 h^{-1}).

Table 2
Influence of S/C on toluene conversion at different temperatures Ni/mayenite (5%) (S.V.: 6000 h^{-1}).

S/C				
Temp.				
	1.4	1.8	2.2	2.6
450 °C	24.3	24.7	28.1	30.3
500 °C	40.4	42.5	44.3	46.0
550 °C	70.5	74.5	77.4	79.7

also the H_2 yield before deactivation was similar to that of in the absence of H_2S, the result was shown in Fig. 11, which also illustrated that life time of catalyst was related with the amount catalyst, as well as the amount of "free" oxygen in the catalyst. By calculation, according to the space velocity and the concentration of H_2S, suppose one S atom substitutes one "free oxygen structure", and the H_2S was absorbed by Ni/mayenite during the experiment, then the amount of "free" oxygen (O_2^- and O_2^{2-}) in catalyst structure was near 0.4 wt%, which was coincident with our previous study [33], the "theoretical" amounts of O_2^- and O_2^{2-} were estimated 0.41 wt% for mayenite

3.3.2. Conversion and selectivity

The detail of toluene conversion and products selectivity on Ni/mayenite (5%) was studied as a function of time in the presence of 500 ppm H_2S at 800 °C, and compared with mayenite, the results were shown in Fig. 12. It found that the toluene conversion and benzene selectivity of mayenite increased gradually with time on stream from starting point, while Ni/mayenite was deactived abruptly after a period time, and also found the same trend in Fig. 11. The possible reason to account for this is that mayenite can absorb sulfur and protect Ni metal site. Only after all the support (mayenite) was poisoned gradually, which will take near 1 h in the experimental condition. After this, the Ni metal will be deactivated very quickly. Because the amount of Ni metal in the catalyst is very less (around 4.31×10^{-5} mol in the experiment), but the flowrate of H_2S is relatively high around 2.45×10^{-6} mol min^{-1}, so the process for Ni metal totally poisoned by H_2S will be less than 20 minutes. If the initial nickel sulfide covered the surface of Ni metal sites and deactivated the Ni site, the time will be less than theoretical value, that is why the time shown in experimental results was shorter, and Ni was deactivated abruptly in Figs. 11 and 12. From the results, it was also judged than the conversion of

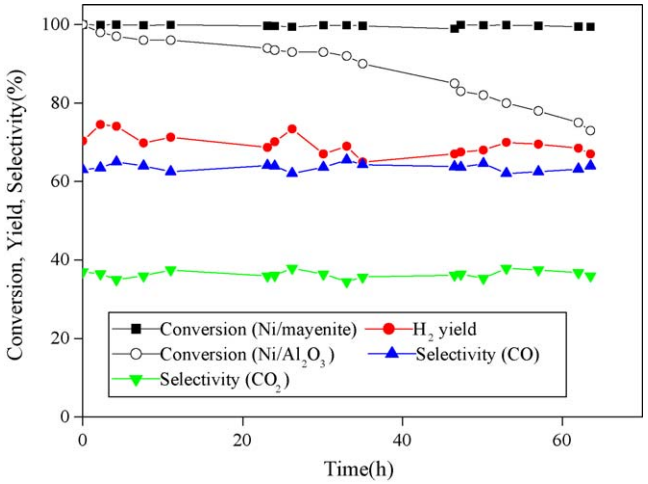

Fig. 9. Toluene conversion, H_2 yield, CO and CO_2 selectivity vs. time (S/C = 1.15, temp. = 800 °C, toluene concentration = 4000 ppm).

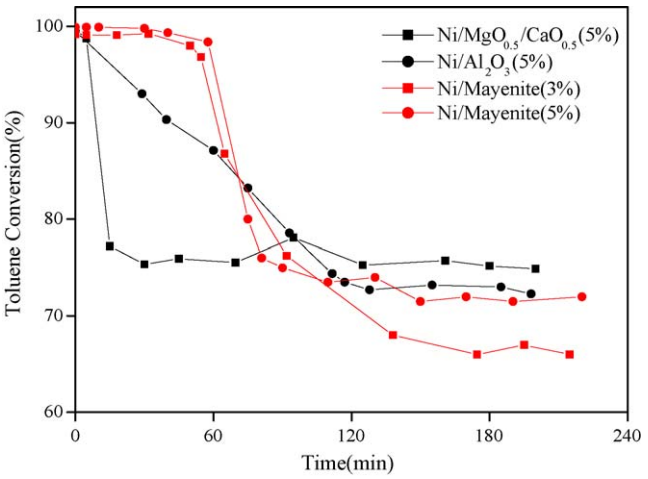

Fig. 10. Toluene conversion vs. time on different catalysts (H_2S: 500 ppm, S.V.: 6000 h^{-1}, temp.: 800 °C).

toluene on Ni/mayenite was still above 70% after the catalyst was poisoned by H_2S, but nearly half of toluene converted to benzene, the selectivity of which reached 40%. The conversion and selectivity were similar to mayenite at the same condition after the catalyst deactived, which showed that Ni metal in the Ni/mayenite totally lost its activity after certain period in the presence of H_2S.

The catalysts before and after reaction were characterized by XRD patterns, and shown in Fig. 13. It was found that all the catalysts before and after reaction still remained the mayenite structure even if reaction undertook longer time (more than 12 h). But for the Ni/mayenite, the Ni/NiO peaks disappeared after reaction in the presence of H_2S, and exited in NiS, Ni_3S_2 sulfide. From the enlarged figure (Fig. 13), a small shift of the mayenite and Ni/mayenite angle was found after reaction. The reasonable explanation is the substitution "free oxygen" by S atom, mayenite ($Ca_{12}Al_{14}O_{33}$) changed to sulfide mayenite ($Ca_{12}Al_{14}O_{32}S$), and still remained the mayenite structure. After this, we studied the toluene selectivity and conversion for fresh mayenite in the

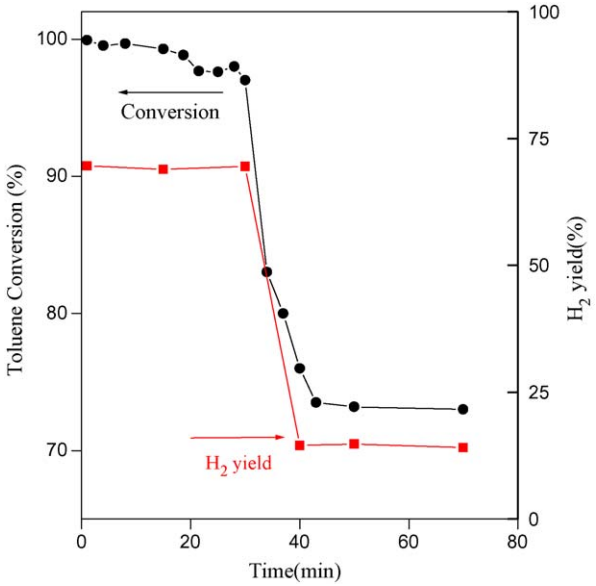

Fig. 11. Toluene conversion and H_2 yield vs. time on Ni/mayenite (5%) (H_2S: 500 ppm, S.V.: 12,000 h^{-1}, temp.: 800 °C).

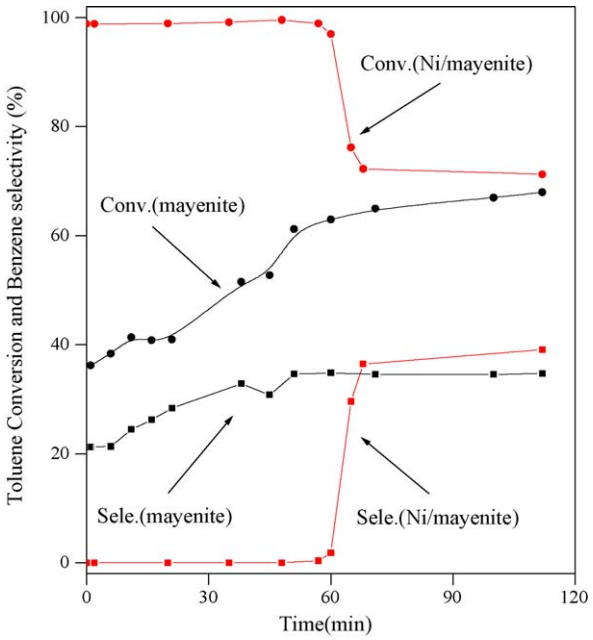

Fig. 12. Toluene conversion and selectivity vs. time on different catalysts (H_2S: 500 ppm, S.V.: 6000 h^{-1}, temp.: 800 °C).

absence of H_2S, and the deactivation mayenite ($Ca_{12}Al_{14}O_{32}S$) in the presence of H_2S (Fig. 14), it found that $Ca_{12}Al_{14}O_{32}S$ exhibited higher toluene conversion comparing to fresh mayenite, but the selectivity of benzene also raised.

3.3.3. Restore of "free oxygen"

From the above research, it can conclude that mayenite can absorb sulfide, protects Ni metal, and then prolongs life time of the catalyst, the reason lies in the "free oxygen" can be substituted by S atom. Based on this, we studied the possibility for the "free oxygen" restore. The deactivation catalysts were flowed by O_2 (20% diluted by Ar) and H_2 (<5% diluted by Ar) respectively for 30 min at 650 °C, then reacted again at the same condition. The results of aging experiments at different temperature for Ni/mayenite (5%) were shown in Fig. 15. It was judged that the performance of the refreshed catalyst only remained a very short time (less than 10 min) at 800 °C. Even at 650 °C, it also only remained around 10 min after treated by O_2 and H_2, which showed that the sulfide catalyst by H_2S was hardly restored, and the sulfide mayenite was more stable than mayenite.

The restore ability of the Ni/mayenite before deactivation was also studied. When the reaction performs 30 min at the same condition, the toluene feed was stopped, and the gas was changed to O_2 (20% diluted by Ar) and H_2 (<5% diluted by Ar) respectively for 30 min at 650 °C, then started toluene steam reforming again. The results were shown in Fig. 16, which illustrated there is no obvious influence on the total life time. It is also proved that the S atom absorbed in the mayenite structure was hardly re-substituted by O_2.

The appearing and disappearing behavior of O_2^{2-} and O_2^- was examined by Raman spectroscopy after reaction with H_2S or oxygen gas at 650 °C. Fig. 17 shows the results of mayenite and Ni/mayenite. The intensity of two Raman bands (880 and 1090 cm^{-1}) of the mayenite and Ni/mayenite decreased after reacted with H_2S, and the intensity of two bands in mayenite was partly restored after reacted with oxygen, but this was not obvious for Ni/mayenite. Between these two species, O_2^- was more preferentially consumed under a H_2S atmosphere. The disappearing and

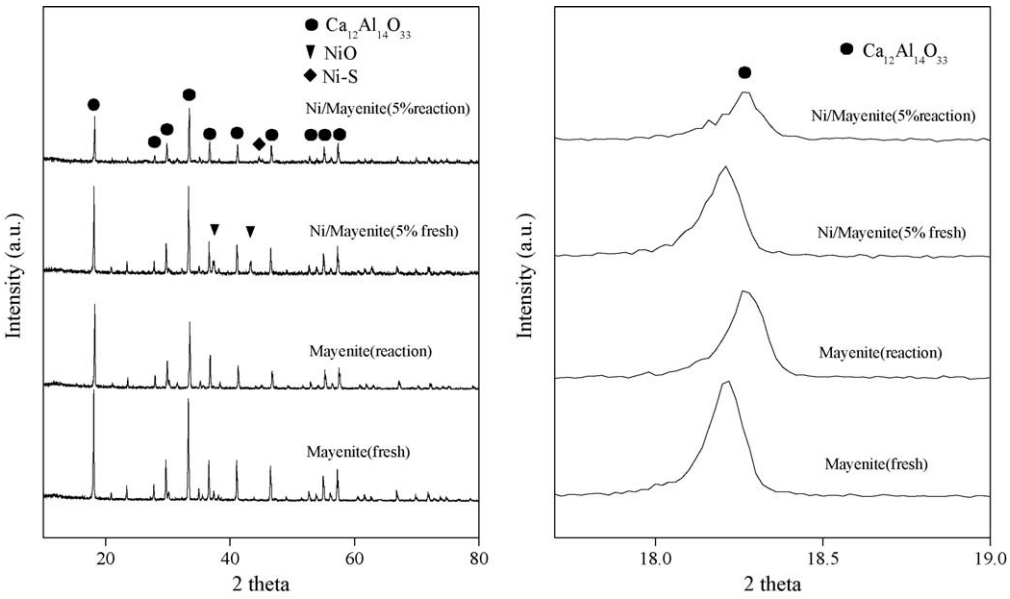

Fig. 13. X-ray diffraction pattern of mayenite and Ni/mayenite before and after reaction.

reproducing behavior of molecular oxygen anions of mayenite was also confirmed from TG measurements in our previous study [33], in which the reduce environment was H_2. Reaction with hydrogen decreased the weight of mayenite, and reaction of oxygen restored their weights.

3.4. Kinetic parameters

It is of interest to conduct kinetic studies in the conditions where heat and mass transfer resistances are absent. The reactor has been considered as plug flow. The apparent rate constant and the apparent activation energy for toluene steam reforming can be expressed in the form:

$$-r_t = kC_t^n C_{H_2O}^m \quad (13)$$

The before mentioned experimental results showed that there is obvious influence of water concentration on conversion of toluene. But at this condition, the water concentration was kept constant, so the disappearance rate of toluene (Eq. (13)) in a binary reaction with H_2O can be expressed as a pseudo-order reaction with respect to only toluene concentration. For tar decomposition reaction-order, some researchers considered that it was less than 1, for example, Jess [34] obtained reaction-order 0.2 for tar cracking model components naphthalene (reaction medium: $H_2 + H_2O$, Ni-catalysts); Devi et al. [35] obtained reaction-order 0.3 for tar decomposition model components naphthalene (reaction medium: $H_2O + CO_2 + CO + H_2$, olivine as catalyst). But summarized the research, it can found that the decomposition rate of tar usually is assumed to the first-order, and also widely accepted in the literature data [36–43], in this study, the toluene reaction was also regarded as first-order reaction, then Eq. (13) can be expressed as

$$-r_t = k_{app}C_t \quad (14)$$

Under plug flow conditions, the apparent rate constant can be calculated as

$$k_{app} = \frac{[-\ln(1 - X_c)]}{\tau} \quad \tau = \frac{W}{\nu_0} \quad (15)$$

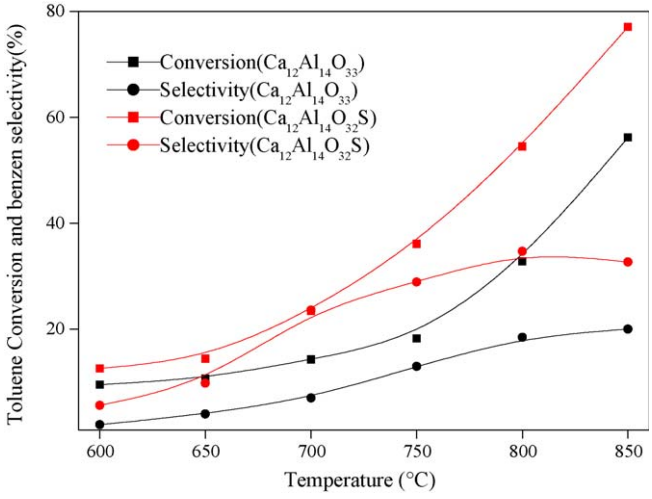

Fig. 14. The conversion and selectivity of mayenite and sulfide mayenite (S.V.: 6000 h^{-1}).

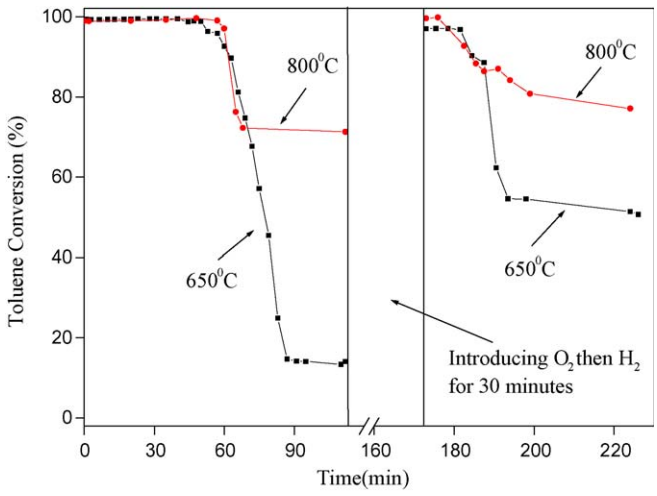

Fig. 15. The restore ability of sulfide Ni/mayenite at different temperatures.

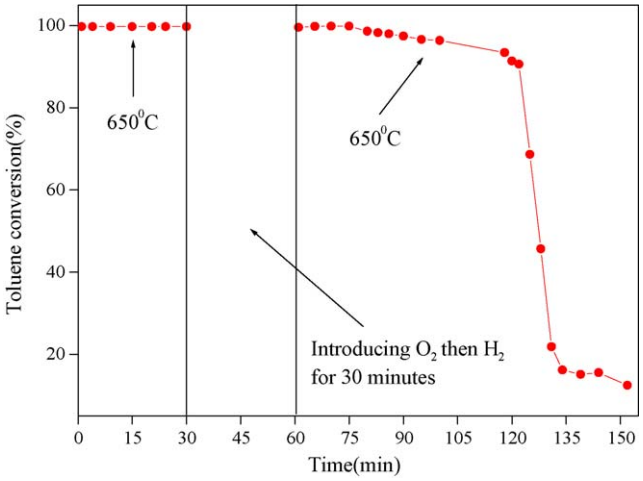

Fig. 16. The "O" restore ability of sulfide Ni/mayenite before total deactivation.

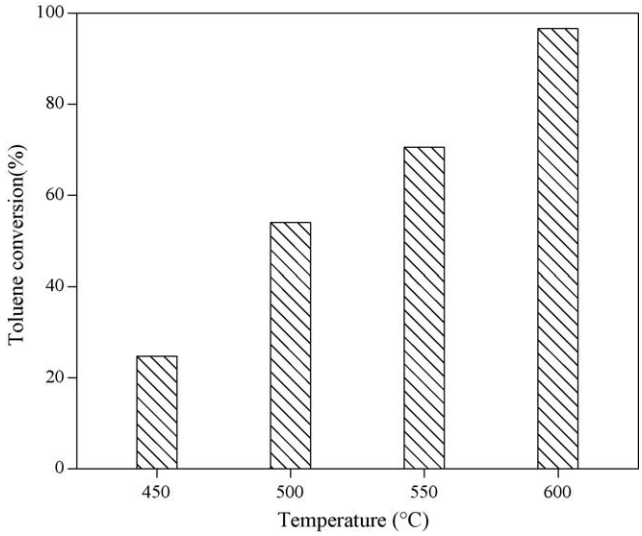

Fig. 18. Temperature effect on toluene steam reforming conversion (T: 450–600 °C, S.V.: 6000 h^{-1}).

The temperature dependency according to Arrhenius's Law can be represented as

$$k_{app} = k_{0,app} e^{-E_{app}/RT} \quad (16)$$

To find the activation energy, experiments were performed in a temperature range of 400–600 °C with gas composition (toluene 4000 ppm diluted by Ar, S/C: 1.9). The effect of temperature on toluene conversion was shown in Fig. 18, then apparent activation energy for toluene conversion over Ni/mayenite (5 wt%) was calculated from Fig. 19, shown in Table 3.

These values are in concordance with values reported by Narvaez et al. [36] for tar steam reforming on commercial nickel based catalyst (BASF G1-25S), performed in air gasifying agent (72 ± 12 kJ mol^{-1}), and 84 ± 6 kJ mol^{-1} over calcined dolomite. Azner et al. [37] found energies between 30 and 97 kJ mol^{-1} for different catalysts with a first-order reaction rate, while Narvaez et al. [38] obtained 72–97 kJ mol^{-1}. Comparatively, Świerczyński et al. [28,39] reported higher activation energy value of 196 kJ mol^{-1} over Ni/olivine at 850 °C. Taralas et al. [40] reported activation energy value of 356 kJ mol^{-1} for toluene thermal destruction in [N_2 + H_2 + H_2O] gas mixture. These comparisons demonstrated the efficiency of the Ni/mayenite catalyst in toluene steam reforming.

On the other hand, some lower activation energy values were reported, 51 kJ mol^{-1} for tar removal reaction on nickel based catalyst by Lv et al. [42], 42–47 kJ mol^{-1} for tar steam reforming on calcined dolomite by Delgado et al. [43]. In fact, the calculated apparent activation energies reported for tar component cracking in the literature varied over a wide range [44,45]. So it is very difficult to compare the data from tar (one lump model) and model compound model studies.

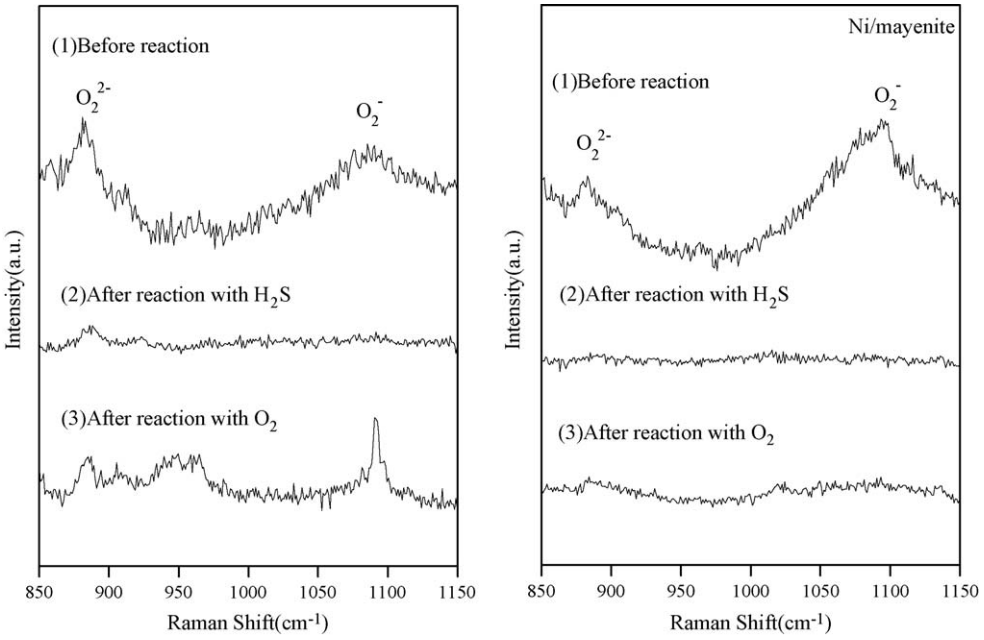

Fig. 17. Raman spectra of mayenite and Ni/mayenite after reaction with H_2S or oxygen gas at 650 °C.

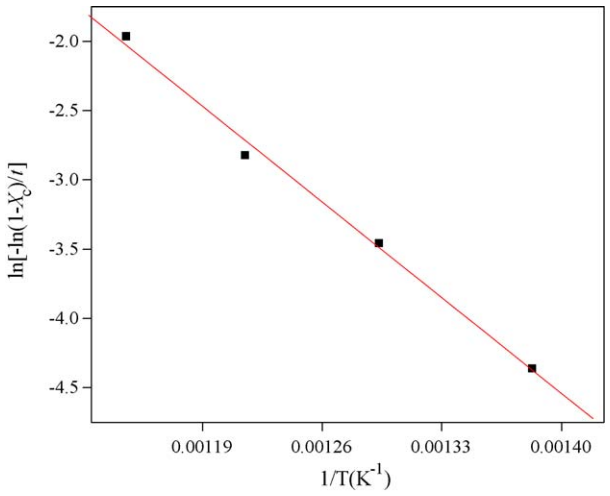

Fig. 19. Arrhenius plot for calculation of apparent activation energy (T: 450–600 °C, S.V.: 6000 h^{-1}).

Table 3
Estimates of the kinetic parameters for toluene steam reforming on Ni/mayenite (Toluene 4000 ppm diluted by argon, S/C: 1.9, temperature from 450 to 600 °C, S.V.: 6000 h^{-1}.).

Parameters	Estimated value
A (h^{-1})	1.06×10^4
E_a (kJ mol^{-1})	82.06

4. Conclusions

One new catalyst ($Ni/Ca_{12}Al_{14}O_{33}$) for biomass tar steam reforming was developed, which has special structure and high "free oxygen" restored property. It exhibited excellent carbon formation resistance and sulfur-tolerant ability.

The influence of the catalyst preparation parameters and operating parameters (reaction temperature, steam to carbon ratio) on activity and products selectivity was examined. The results confirmed that the new developed catalyst showed a high toluene reforming activity even 1% Ni metal loading and long-time durability exhibited superior resistance to carbon poisoned.

$Ni/Ca_{12}Al_{14}O_{33}$ shows excellent H_2S tolerance property comparing to other catalysts such as $Ni/MgO_{0.5}/CaO_{0.5}$, Ni/Al_2O_3. Raman spectra reveals sulfur-tolerant property lies in that "free oxygen" in the structure of the catalysts can be substituted by sulfur, and prolongs Ni life time. But experiments showed that the sulfide mayenite was hardly restored by flowing O_2.

Lastly, the activation energy of 82.06 kJ mol^{-1} for toluene steam reforming process was calculated by the proposed kinetic model.

Acknowledgements

The authors gratefully acknowledge the postdoctoral fellowship No. P08408 along with Grant-in-aid No. 20-08408 awarded from Japan Society for the Promotion of Science (JSPS).

References

[1] B. Christopher, J. Field, C. Elliott, B.L. David, Trends Ecol. Evol. 23 (2008) 65–72.
[2] J. Han, H. Kim, Renew. Sustain. Energy Rev. 12 (2008) 397–416.
[3] D. Duprez, Appl. Catal. A 82 (1992) 111–157.
[4] J. Sehested, Catal. Today 111 (2006) 103–110.
[5] E. Nikolla, J. Schwank, S. Linic, J. Catal. 250 (2007) 85–93.
[6] X.L. Zhu, P.P. Huo, Y.P. Zhang, D.G. Cheng, Appl. Catal. B 81 (2008) 132–140.
[7] K. Engelen, Y. Zhang, D.J. Draelants, G.V. Baron, Chem. Eng. Sci. 58 (2003) 665–670.
[8] J. Srinakruang, K. Sato, T. Vitidsant, K. Fujimoto, Catal. Commun. 6 (2005) 437–440.
[9] A.C. Basagiannis, X.E. Verykios, Catal. Today 127 (2007) 256–264.
[10] A.C. Basagiannis, X.E. Verykios, Appl. Catal. B 82 (2008) 77–88.
[11] J.H. Jeong, J.W. Lee, D.J. Seo, Y. Seo, W.L. Yoon, D.K. Lee, D.H. Kim, Appl. Catal. A 302 (2006) 151–156.
[12] K. Sato, K. Fujimoto, Catal. Commun. 8 (2007) 1697–1701.
[13] K. Oka, T. Nishiguchi, H. Kanai, K. Utani, S. Imamura, Appl. Catal. A 309 (2006) 187–191.
[14] J. Nishikawa, T. Miyazawa, K. Nakamura, M. Asadullah, K. Kunimori, K. Tomishige, Catal. Commun. 9 (2008) 195–201.
[15] M.E. Domine, E.E. Iojoiu, T. Davidian, N. Guilhaume, C. Mirodatos, Catal. Today 133 (2008) 565–573.
[16] M. Nurunnabi, K. Fujimoto, K. Suzuki, B. Li, S. Kado, K. Kunimori, K. Tomishige, Catal. Commun. 7 (2006) 73–78.
[17] F. Aupretre, C. Descorme, D. Duprez, D. Casanave, D. Uzio, J. Catal. 233 (2005) 464–477.
[18] T. Davidian, N. Guilhaume, E.E. Iojoiu, H. Provendier, C. Mirodatos, Appl. Catal. B 73 (2007) 116–127.
[19] D.H. Kim, J.S. Kang, Y.J. Lee, N.K. Park, Y.C. Kim, S.I. Hong, D.J. Moon, Catal. Today 136 (2008) 228–234.
[20] A.M. Azad, M.J. Duran, A.K. McCoy, M.A. Abraham, Appl. Catal. A 332 (2007) 225–236.
[21] S.H. Seok, S.H. Choi, E.D. Park, S.H. Han, J.S. Lee, J. Catal. 209 (2002) 6–15.
[22] N. Eranda, S. Johannes, L. Suljo, J. Catal. 250 (2007) 85–93.
[23] M.C. Demicheli, D. Duprez, J. Barbier, O.A. Ferretti, E.N. Ponzi, J. Catal. 145 (1994) 437–449.
[24] F. Frusteri, S. Freni, V. Chiodo, L. Spadaro, G. Bonura, S. Cavallaro, J. Power Sources 132 (2004) 139–144.
[25] A. Nandini, K.K. Pant, S.C. Dhingra, Appl. Catal. A 290 (2005) 166–174.
[26] S. Fujita, H. Nakano, K. Suzuki, T. Mori, H. Masuda, Catal. Lett. 106 (2006) 139–143.
[27] S. Fujita, K. Suzuki, M. Ohkawa, T. Mori, Y. Lida, Y. Miwa, H. Masuda, S. Shimada, Chem. Mater. 15 (2003) 255–263.
[28] D. Świerczyński, S. Libs, C. Courson, A. Kiennemann, Appl. Catal. B 74 (2007) 211–222.
[29] J. Corella, J.M. Toledo, R. Padilla, Energy Fuels 18 (2004) 713–720.
[30] J.N. Kuhn, Z.K. Zhao, A. Senefeld-Naber, L.G. Felix, R.B. Slimane, C.W. Choi, U.S. Ozkan, Appl. Catal. A 341 (2008) 43–49.
[31] T.J. Wang, J. Chang, P.M. Lv, Energy Fuels 19 (2005) 22–27.
[32] L. Palacios, A. Cabeza, S. Bruque, S.G. Granda, M.A.G. Aranda, Inorg. Chem. 47 (2008) 2661–2667.
[33] S. Fujita, H. Nakano, K. Suzuki, T. Mori, H. Masuda, Catal. Lett. 106 (2006) 3–4.
[34] A. Jess, Chem. Eng. Process 35 (1996) 487–494.
[35] L. Devi, K.J. Ptasinski, F.J.J.G. Janssen, Ind. Eng. Chem. Res. 44 (2005) 9096–9104.
[36] I. Narvaez, J. Corella, A. Orio, Ind. Eng. Chem. Res. 36 (1997) 317–327.
[37] M.P. Azner, M.A. Caballero, J. Gil, J.A. Martin, Ind. Eng. Chem. Res. 37 (1998) 2668–2680.
[38] I. Narvaez, J. Corella, A. Orio, Ind. Eng. Chem. Res. 36 (2) (1997) 317–327.
[39] D. Świerczyński, C. Courson, A. Kiennemann, Chem. Eng. Process 47 (2008) 508–513.
[40] G. Taralas, M.G. Kontominas, X. Katatsios, Energy Fuels 17 (2003) 329–337.
[41] C.S. Li, Y. Yamamoto, M. Suzuki, D. Hirabayashi, K. Suzuki, J. Therm. Anal. Calorim., (2008) doi: 10.1007/s10973-008-9126-8.
[42] P. Lv, Z. Yuan, C. Wu, L. Ma, Y. Chen, N. Tsubaki, et al. Energy Convers. Manage. 48 (2007) 1132–1139.
[43] J. Delgado, M.P. Aznar, J. Corella, Ind. Eng. Chem. Res. 36 (1997) 1535–1543.
[44] C. Li, K. Suzuki, Renew Sustain Energy Rev. (2008), doi:10.1016/j.rser.2008.01.009.
[45] J. Corella, M.A. Caballero, M. Aznar, C. Brage, Ind. Eng. Chem. Res. 42 (2003) 3001–3011.